J. Chem. Thermodynamics 107 (2017) 79–84

Contents lists available at ScienceDirect

J. Chem. Thermodynamics

journal homepage: www.elsevier.com/locate/jct

# Surface thermodynamics of DMA2P, DMA2P-MEA and DMA2P-PZ aqueous solutions

Dong Fu *, LeMeng Wang, XiangFeng Tian

*School of Environmental Science and Engineering, North China Electric Power University, Baoding 071003, People's Republic of China*

ARTICLE INFO

*Article history:*
Received 6 November 2016
Received in revised form 5 December 2016
Accepted 23 December 2016
Available online 26 December 2016

*Keywords:*
Surface tension
Surface thermodynamics
DMA2P
MEA
PZ

ABSTRACT

The surface tension ($\gamma$) of 1-dimethylamino-2-propanol (DMA2P), DMA2P-monoethanolamine (MEA), and DMA2P-piperazine (PZ) aqueous solutions was measured by using the BZY-1 surface tension meter. The temperature ranged from 303.2 K to 323.2 K. The mass fractions of DMA2P, MEA and PZ respectively ranged from 0.30 to 0.50, 0.05 to 0.15 and 0.025 to 0.075. An equation was proposed to model the surface tension and the calculated results agreed well with the experiments. The surface thermodynamics including surface enthalpy and surface entropy were determined and their concentration dependence was analysed.



## 1. Introduction

Considerable attentions have been attracted on climate change and environmental problems and the reduction of $CO_2$ has become a global issue [1,2]. Post combustion $CO_2$ capture using amine as absorbent is considered to be very promising because of high efficiency and selectivity [3–8]. Conventional amines, including primary amine monoethanolamine (MEA), secondary amine diethanolamine (DEA), tertiary amine N-methyldiethanolamine (MDEA) and diamine piperazine (PZ) are effective for capturing $CO_2$ from a variety of industrial processes [9–12]. However, the conventional amines have many drawbacks, *e.g.*, the absorption capacity of primary and secondary amines aqueous solution is relatively low but the energy consumption in regeneration process is high, and the absorption of $CO_2$ in tertiary amines aqueous solution is quite slow. Due to the drawbacks of conventional amines, the blended amines of tertiary amines (MDEA) with primary, secondary amines and diamines attracted great attentions in recent decades. It has been well documented that adding activators such as MEA, DEA or PZ into MDEA aqueous solution preserves the high rate of the reaction of activators with $CO_2$, and the low enthalpy of the reaction of MDEA with $CO_2$, hence lead to higher absorption rates in the absorber column, yet lower heat of regeneration in the stripper section [13–17].

Recently, DMA2P has attracted increasing attention in $CO_2$ capture process due to its good absorption performances such as large absorption capacity [18] and high absorption rates [19]. Compared with MDEA, DMA2P also has one nitrogen group in its molecular structure, but there are less sterically hindered substituents on to N-atom, which enhances the absorption rate and cyclic capacity for $CO_2$ capture. For example, the absorption amount ($gCO_2 \cdot L^{-1}$ aqueous solution) and absorption rate of $CO_2$ ($gCO_2 \cdot L^{-1}$ aqueous solution/min) in MDEA and DMA2P aqueous solutions are respectively 55, 1.56 and 92, 2.24 under same operation conditions [18]. By far, there are some studies on the absorption of $CO_2$ in DMA2P aqueous solution, such as absorption capacity, absorption heat, absorption rate, reaction kinetics, and density [20–25]. Besides the aforementioned characteristics, surface properties such as surface tension, surface entropy and surface enthalpy are also important. Surface tension is highly important for the gas-liquid mass transfer process. It can significantly affect the absorption efficiency because both the penetration of $CO_2$ molecules from the gas phase to the liquid phase and the enhancement of the absorption are closely related to it. The knowledge of surface entropy and surface enthalpy is required when exploring further relationships between the surface and bulk properties of aqueous solutions, *e.g.*, the molecular force and surface structure of the aqueous solution can be inferred according to the variation of surface entropy and surface enthalpy, and the analysis of surface entropy and surface enthalpy can provide important information on the character of surface structure. In recent years, there are some experimental and theoretical work concerning the surface tension, surface

* Corresponding author.
*E-mail address:* fudong@tsinghua.org.cn (D. Fu).

http://dx.doi.org/10.1016/j.jct.2016.12.022
0021-9614/

entropy and surface enthalpy of aqueous solutions containing amines and their blends [26–39]. However, experimental and theoretical studies on the surface tension, surface entropies and surface enthalpies of DMA2P, DMA2P-MEA and DMA2P-PZ aqueous solutions are rare.

The main purposes of this work are to (1) experimentally determine the surface tension of DMA2P, DMA2P-MEA and DMA2P-PZ aqueous solutions; (2) correlate the surface tension by using thermodynamic equations and determine the surface entropies and surface enthalpies; (3) demonstrate the effects of temperature and mass fractions of amines on the surface thermodynamics. To this end, the surface tension was measured at temperatures ranging from 303.2 K to 323.2 K. The mass fractions of DMA2P, MEA and PZ respectively ranged from 0.3 to 0.5, 0.05 to 0.15 and 0.025 to 0.075. Besides experimental work, an equation is proposed in this work to model the surface tension. The surface enthalpies and surface entropies were calculated, and their concentration dependence was also analysed.

## 2. Experimental

### 2.1. Materials

Chemicals used for this work are detailed in Table 1. All the chemicals were used as received, without any purification. The water contents (in mass percent) of DMA2P, MEA and PZ are respectively 0.06%, 0.06% and 0.05% (determined by using the Karl Fischer method, as stated by the supplier). An analytical balance (Jingtian FA1604A) with an accuracy of 0.1 mg was used to weigh all required chemicals. However, taking the purities and water content into account, the uncertainties of the mass fractions of DMA2P, MEA and PZ are respectively $u(w_{DMA2P}) = \pm 0.005$, $u(w_{MEA}) = \pm 0.002$ and $u(w_{PZ}) = \pm 0.002$. Aqueous solutions of DMA2P, DMA2P-MEA, and DMA2P-PZ were prepared by adding deionized water (Electrical resistivity >15 MΩ·cm at 298 K) obtained from the Heal Force ROE (Reverse Osmosis Electrodeionization)-100 apparatus to the weighed quantities of amines.

### 2.2. Apparatus and procedure

The surface tension was measured by using the BZY-1 surface tension meter produced by Shanghai Hengping Instrument Factory. The BZY-1 meter employs the Wilhemy plate principle, *i.e.*, the maximum tensile force competing with the surface tension is measured when the bottom edge is parallel to the interface and just touches the liquid. The measurement ranges for temperature and surface tension are respectively (268.15 to 383.15) K and (0.1–400.0) $mN{\cdot}m^{-1}$. The uncertainty is ±0.1 $mN{\cdot}m^{-1}$. The size-volume of the different samples used in the BZY-1 meter is 20 mL. During the experiments, the copper pan in the host of the BZY-1 meter is connected with the thermostatic bath (CH-1006, uncertainty is ±0.1 K). Via the circulation of the water, the temperature of the water in the copper pan is kept the same as that in the thermostatic bath. The aqueous solution is put into the solution container immersed in the copper pan and its temperature can be measured by a thermocouple. The scale reading of the thermocouple has been well calibrated by a mercury thermometer.

## 3. Results and discussion

### 3.1. Surface tension

To verify the reliability of the equipment, the surface tension of water was measured under $T = 298.2$ K. The value obtained is 71.9 $mN{\cdot}m^{-1}$. This value was compared with that (72.0 $mN{\cdot}m^{-1}$) presented in the work of Fu et al. [26] and Vázquez et al. [32], and the deviation is 0.14%, indicating that the equipment used in this work is reliable.

The experimental results of the surface tension of DMA2P, DMA2P-MEA and DMA2P-PZ aqueous solutions are respectively shown in Tables 2–4. Besides experimental measurements, models that can correctly calculate the surface tension of concerned systems are also important. In this work, the surface tension of DMA2P, DMA2P-MEA and DMA2P-PZ aqueous solutions are formulated as follows:

$$\gamma^{aq} = \gamma^{0} + \gamma' \tag{1}$$

in which $\gamma^0$ and $\gamma'$ are expressed as:

$$\gamma^{0} = x_1\gamma_1 + x_2\gamma_2 + x_3\gamma_3 \tag{2}$$

$$\gamma' = x_1x_2G_{12} + x_1x_3G_{13} + x_2x_3G_{23} \tag{3}$$

where the subscripts 1, 2 and 3 stand for DMA2P, activator (MEA or PZ) and water, respectively; $x_i$ is the mole fraction of component $i$ in the aqueous solution, $\gamma_i$ is the surface tension of pure component $i$, which can be expressed as a function of the temperature by fitting to the experimental data. $G_{ij}$ is expressed as a function of temperature and mass fraction $w_i$, with 2 adjustable model parameters for binary mixtures and 6 adjustable model parameters for ternary mixtures:

$$G_{13} = \frac{a_{13}}{w_{DMA2P}} + b_{13} \times T \tag{4}$$

$$G_{23} = \frac{a_{23}}{w_{MEA/PZ}} + b_{23} \times T \tag{5}$$

$$G_{12} = \frac{a_{12}}{(w_{DMA2P} + w_{MEA/PZ})/2} + b_{12} \times T \tag{6}$$

The model parameters $a_{ij}$ and $b_{ij}$ can be obtained by fitting to the experimental data. The objective function (the average relative deviation, ARD) is defined as:

$$ARD = \sum_{i=1}^{n}\left(1 - \gamma^{cal}/\gamma^{exp}\right) \times 100\%/n \tag{7}$$

where the superscripts 'exp' and 'cal' respectively stand for the experimental and calculated data, $n$ is the number of experimental points.

For DMA2P aqueous solutions, the model parameters were regressed from the experimental surface tension of DMA2P aque-

**Table 1**
Sample description.

| Chemical name | CAS | Purity (mole fraction, as stated by the supplier) | Water content(mass percent, as stated by the supplier) | Source |
|---|---|---|---|---|
| DMA2P | 108-16-7 | $x \geqslant 0.98$ | 0.06% | TCI Reagent |
| MEA | 141-43-5 | $x \geqslant 0.995$ | 0.06% | Aladdin Reagent |
| PZ | 110-85-0 | $x \geqslant 0.995$ | 0.05% | Sinopharm Chemical Reagent |
| Water | 7732-18-5 | Electrical resistivity > 15 MΩ cm at $T = 298$ K | | Heal force ROE-100 apparatus |

**Table 2**
Surface tensions ($\gamma$) of DMA2P aqueous solutions under different mass fractions of DMA2P ($w_{DMA2P}$). Pressure ($p$) = 101 kPa.[a]

| $w_{DMA2P}$ | $\gamma$/(mN·m$^{-1}$) | | |
|---|---|---|---|
| | $T$ = 303.2 K | 313.2 K | 323.2 K |
| 0.100 | 45.1 | 43.4 | 41.9 |
| 0.200 | 39.9 | 37.8 | 36.2 |
| 0.300 | 36.2 | 34.6 | 33.2 |
| 0.400 | 33.6 | 32.3 | 30.8 |
| 0.500 | 31.6 | 30.4 | 29.1 |
| 0.600 | 29.8 | 28.8 | 27.4 |
| 0.700 | 28.4 | 27.3 | 26.2 |
| 0.800 | 27.1 | 26.0 | 24.6 |
| 0.900 | 25.9 | 24.6 | 23.5 |
| 1.000 | 24.0 | 22.7 | 21.4 |

[a] Standard uncertainties $u$ are $u(T)$ = 0.1 K; $u(w_{DMA2P})$ = ± 0.005; $u(\gamma)$ = 0.15 mN·m$^{-1}$; $u(p)$ = 5 kPa.

ous solutions, with $w_{DMA2P}$ ranging from 0.3 to 0.7. It is worth noting that the mass fraction dependence of the surface tension of DMA2P aqueous solutions is similar to that of the surfactant aqueous solutions, *i.e.*, when the values of $w_{DMA2P}$ are small, the surface tension decreases monotonically and rapidly with increasing $w_{DMA2P}$. Exceeding a certain value, the surface tension tends to change slightly. The present model is unable to accurately describe such a tendency of surface tension. As $w_{DMA2P}$ in both DMA2P-PZ and DMA2P-MEA aqueous solutions ranges from 0.3 to 0.5, it is reasonable to regress the model parameters of DMA2P by fitting to the experiments corresponding to $w_{DMA2P}$ ranging from 0.3 to 0.7. The optimized results are $a_{13}$ = −190.0 and $b_{13}$ = 0.41. The ARD is 1.65%. For DMA2P-MEA aqueous solutions, the model parameters were regressed from the experimental surface tension of DMA2P-MEA aqueous solutions. The optimized results are $a_{23}$ = −1.51, $b_{23}$ = 0.298, $a_{12}$ = −2.57 and $b_{12}$ = −0.432. The ARD is 0.88%. When regressing the model parameters of DMA2P-PZ aqueous solution, $\gamma_2$ can be treated as a constant because PZ appears solid state at room temperatures. $\gamma_2$ = 31.94 mN·m$^{-1}$ was directly taken from the previous work [27]. The optimized results are $a_{23}$ = −0.914, $b_{23}$ = 0.549, $a_{12}$ = 37.6 and $b_{12}$ = −1.68. The ARD is 1.09%.

Fig. 1 shows the temperature and $w_{DMA2P}$ dependences of the surface tension of DMA2P aqueous solutions, indicating that the surface tension decreases with the increases of both $w_{DMA2P}$ and temperature. Fig. 2 shows the influence of the mass fraction of activator ($w_{MEA}$ or $w_{PZ}$) on the surface tension of DMA2P-MEA and DMA2P-PZ aqueous solutions. From this figure, one may find that at given temperature and given $w_{DMA2P}$, the surface tension monotonically decreases with the increase of $w_{MEA}$ or $w_{PZ}$. The agreement between the experiments and calculations is satisfactory. Fig. 3 shows the temperature dependence of the surface tension of DMA2P-MEA and DMA2P-PZ aqueous solutions. From this figure, one may find that at given $w_{DMA2P}$ and given $w_{MEA}$ or $w_{PZ}$, the surface tension decreases almost linearly with the increase of temperature. Fig. 4 shows the comparison between the surface tension of DMA2P-MEA and DMA2P-PZ aqueous solutions. One finds that at given $w_{MEA}$ or $w_{PZ}$ and temperature, the surface tension of DMA2P-MEA and DMA2P-PZ aqueous solution decrease with the increase of $w_{DMA2P}$. One may also find that at given $w_{DMA2P}$ and temperature, the surface tension of DMA2P-PZ was smaller than those of DMA2P-MEA aqueous solutions at $w_{MEA}$ = $w_{PZ}$, indicating that PZ is able to decrease the surface tension of DMA2P aqueous solutions more significantly than MEA.

### 3.2. Surface thermodynamics

The surface tension can be used to estimate other surface thermodynamics including surface entropy $S^s$ and surface enthalpy $H^s$, which can be formulated as following [40–45]:

$$S^s = -\left(\frac{\partial \gamma^{aq}}{\partial T}\right)_{x,P} \tag{8}$$

$$H^s = \gamma - T\left(\frac{\partial \gamma^{aq}}{\partial T}\right)_{x,P} \tag{9}$$

In the previous work of Maham et al. [28,29] and Gliński et al. [40–43], the surface tension of aqueous solution was formulated as a linear function of temperature, *i.e.*, $\gamma^{aq} = K_1 + K_2T$, thus at given mass fractions of amines, the surface entropy and surface enthalpy are respectively – $K_2$ and $K_1$. Since the proposed model (Eqs. (1)–(6)) can satisfactorily fit the surface tension, we calculated the surface thermodynamics by combining Eqs. (1)–(6) with Eqs. (8) and (9). The surface entropies and enthalpies of DMA2P aqueous solutions are shown in Fig. 5. Results show that these surface thermodynamics firstly decrease and then increase rapidly at the water-poor region ($w_{DMA2P}$ > 0.9), which is similar to the trends observed in the work of Gliński et al. [40,43] for isobutylamine aqueous solutions [40] and tert-butanol aqueous solutions [43]. Such a phenomenon has been interpreted by Barbas et al. [46] for aqueous solution of amphiphiles, that there exists hydration in the case of very low water concentrations. A considerable fraction of the individual water molecules in the hydration prefer to interact with the hydrophobic groups rather than the hydrophilic groups, thus increasing the surface entropy and surface enthalpy values. Also presented in Fig. 5 are the surface entropies and surface enthalpies obtained by combining $\gamma^{aq} = K_1 + K_2T$ with Eqs. (8) and (9). Comparison showed when the surface tension was formulated as a linear function of temperature, higher surface entropies and surface

**Table 3**
Surface tensions ($\gamma$) of DMA2P-MEA aqueous solutions under different mass fractions of DMA2P ($w_{DMA2P}$) and MEA ($w_{MEA}$). Pressure ($p$) = 101 kPa.[a]

| $w_{DMA2P}$ | $w_{MEA}$ | $\gamma$/(mN·m$^{-1}$) | | |
|---|---|---|---|---|
| | | $T$ = 303.2 K | 313.2 K | 323.2 K |
| 0.300 | 0.050 | 35.6 | 34.2 | 32.9 |
| | 0.100 | 35.3 | 33.9 | 32.6 |
| | 0.150 | 35.0 | 33.6 | 32.3 |
| 0.400 | 0.050 | 32.9 | 31.8 | 30.6 |
| | 0.100 | 32.6 | 31.5 | 30.4 |
| | 0.150 | 32.2 | 31.1 | 30.0 |
| 0.500 | 0.050 | 31.0 | 29.9 | 28.9 |
| | 0.100 | 30.6 | 29.5 | 28.5 |
| | 0.150 | 30.1 | 29.1 | 28.1 |

[a] Standard uncertainties $u$ are $u(T)$ = 0.1 K; $u(w_{DMA2P})$ = ± 0.005; $u(w_{MEA})$ = ± 0.002; $u(\gamma)$ = 0.20 mN·m$^{-1}$; $u(p)$ = 5 kPa.

**Table 4**
Surface tensions ($\gamma$) of DMA2P-PZ aqueous solutions under different mass fractions of DMA2P ($w_{DMA2P}$) and PZ ($w_{PZ}$). Pressure ($p$) = 101 kPa.[a]

| $w_{DMA2P}$ | $w_{PZ}$ | $\gamma$/(mN·m$^{-1}$) | | |
|---|---|---|---|---|
| | | $T$ = 303.2 K | 313.2 K | 323.2 K |
| 0.300 | 0.025 | 35.9 | 34.4 | 33.0 |
| | 0.050 | 35.6 | 34.1 | 32.7 |
| | 0.075 | 35.2 | 33.7 | 32.3 |
| 0.400 | 0.025 | 33.2 | 31.9 | 30.6 |
| | 0.050 | 32.8 | 31.6 | 30.3 |
| | 0.075 | 32.4 | 31.2 | 30.0 |
| 0.500 | 0.025 | 31.2 | 30.0 | 28.8 |
| | 0.050 | 30.8 | 29.7 | 28.5 |
| | 0.075 | 30.5 | 29.4 | 28.2 |

[a] Standard uncertainties $u$ are $u(T)$ = 0.1 K; $u(w_{DMA2P})$ = ± 0.005; $u(w_{PZ})$ = ± 0.002; $u(\gamma)$ = 0.20 mN·m$^{-1}$; $u(p)$ = 5 kPa.

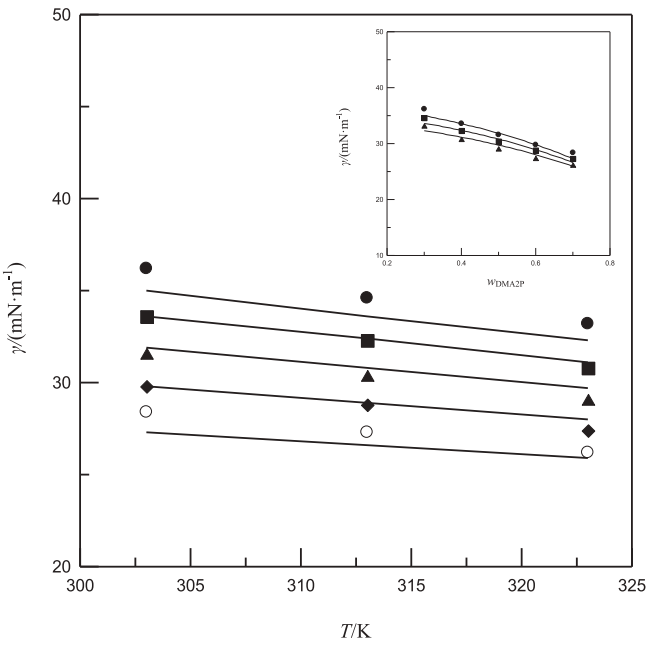


**Fig. 1.** Temperature and $w_{DMA2P}$ (insert plot) dependences of the surface tension of DMA2P aqueous solutions. Main plot: ● $w_{DMA2P}$ = 0.30; ■ $w_{DMA2P}$ = 0.40; ▲ $w_{DMA2P}$ = 0.50; ◆ $w_{DMA2P}$ = 0.60; ○ $w_{DMA2P}$ = 0.70; Insert plot: ● $T$ = 303.2 K; ■ $T$ = 313.2 K; ▲ $T$ = 323.2 K. Symbols: experimental values from this work. Lines: calculated values.

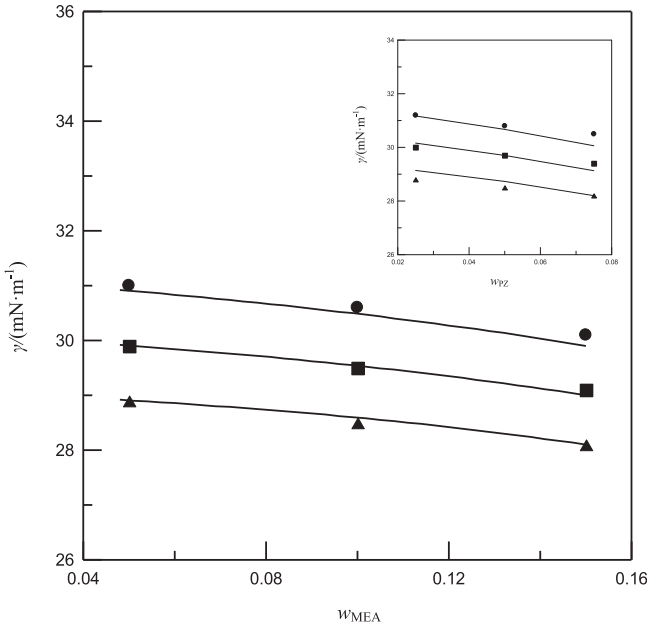


**Fig. 2.** $w_{MEA}$ or $w_{PZ}$ dependence of the surface tension of DMA2P-MEA and DMA2P-PZ (insert plot) aqueous solutions. Main plot: $w_{DMA2P}$ = 0.50, ● $T$ = 303.2 K; ■$T$ = 313.2 K; ▲$T$ = 323.2 K; Insert plot: $w_{DMA2P}$ = 0.50, ● $T$ = 303.2 K; ■$T$ = 313.2 K; ▲$T$ = 323.2 K. Symbols: experimental values from this work. Lines: calculated values.

enthalpies can be obtained, and both the surface entropies and surface enthalpies decrease rapidly at low concentration and they remain practically constant for the rest of the solutions. Similar trends were observed for MDEA aqueous solutions in the work of Maham and Mather [29].

Fig. 6 shows the influence of $w_{DMA2P}$ on the surface thermodynamics of DMA2P-MEA and DMA2P-PZ aqueous solutions, indicating that the surface entropies and surface enthalpies decrease with the increase of $w_{DMA2P}$ at given $w_{MEA}$ or $w_{PZ}$. Fig. 7 shows the influence of the mass fraction of activator ($w_{MEA}$ or $w_{PZ}$) on the surface thermodynamics of DMA2P-MEA and DMA2P-PZ aqueous solutions, indicating that at given $w_{DMA2P}$, the surface entropies and surface enthalpies decrease with the increase of $w_{MEA}$ or $w_{PZ}$. Moreover, comparison shows that PZ is able to decrease the surface thermodynamics of DMA2P aqueous solutions much more significantly than MEA. Such phenomenon may be interpreted by the fact documented in the work of Maham and Mather [29], *i.e.*, for MDEA and MEA aqueous solutions, the molecular structure especially the number of end alkyl groups play very important role in the surface thermodynamics and the increase of end alkyl group may drop the surface thermodynamics of the corresponding aqueous solutions. For DMA2P-PZ and DMA2P-MEA aqueous solutions investigated in this work, it seems the decrease of the surface thermodynamics is dependent on the number of nitrogen groups in PZ and MEA molecules, the more is the nitrogen group, the lower is the surface thermodynamics. For example, there are respectively one and two nitrogen groups in MEA and PZ molecules, thus PZ is able to decrease the surface thermodynamics of DMA2P aqueous solutions more significantly.

## 4. Conclusions

In this work, the surface tension of DMA2P, DMA2P-MEA, and DMA2P-PZ aqueous solutions were measured by using the BZY-1 surface tension meter and modelled by using a thermodynamic equation. The effects of temperature and mass fractions of amines on the surface tension were demonstrated. The surface thermodynamic properties including surface entropy and surface enthalpy were calculated and their concentration dependences were analysed. Our results show that:

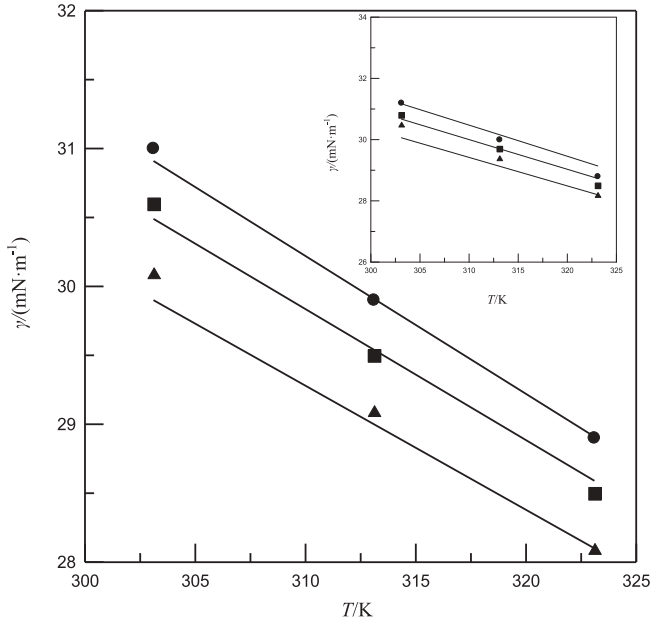


**Fig. 3.** Temperature dependence of the surface tension of DMA2P-MEA and DMA2P-PZ (insert plot) aqueous solutions. Main plot: $w_{DMA2P}$ = 0.50, ● $w_{MEA}$ = 0.05; ■ $w_{MEA}$ = 0.10; ▲ $w_{MEA}$ = 0.15; Insert plot: $w_{DMA2P}$ = 0.50, ● $w_{PZ}$ = 0.025; ■ $w_{PZ}$ = 0.05; ▲ $w_{PZ}$ = 0.075. Symbols: experimental values from this work. Lines: calculated values.

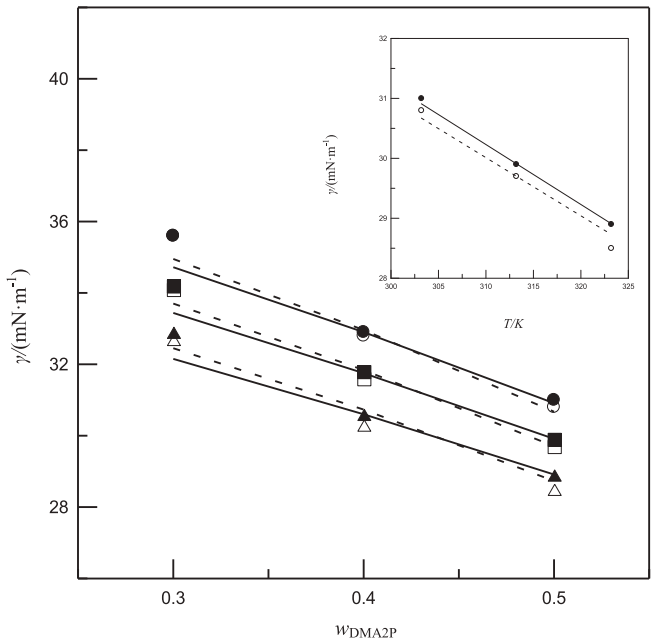


**Fig. 4.** Comparison between the surface tension of DMA2P-MEA (— and solid symbols) aqueous solutions and DMA2P-PZ (— and hollow symbols) aqueous solutions. Main plot: $w_{MEA} = w_{PZ}$ = 0.05, ●○ $T$ = 303.2 K; ■□ $T$ = 313.2 K; ▲△$T$ = 323.2 K; insert plot: $w_{DMA2P}$ = 0.5, ● $w_{MEA}$ = 0.05; ○$w_{PZ}$ = 0.05. Symbols: experimental values from this work. Lines: calculated values.

(1) The increases of temperature and mass fractions of amines tend to decrease the surface tension. The surface tension of DMA2P-MEA and DMA2P-PZ aqueous solutions decreases almost linearly with increasing temperature;
(2) At a given $w_{DMA2P}$ and temperature, the surface tension of DMA2P-PZ is slightly smaller than those of DMA2P-MEA aqueous solutions;

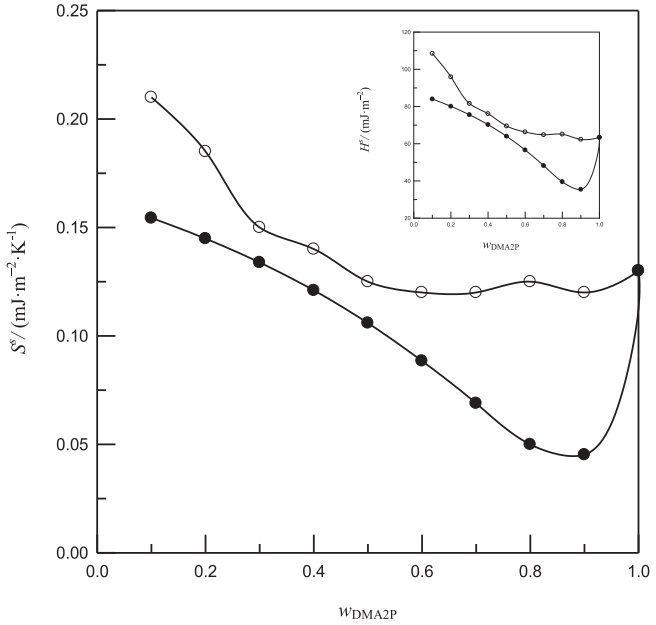


**Fig. 5.** $w_{DMA2P}$ dependence of the surface entropies and enthalpies (insert plot) of DMA2P aqueous solutions. Symbols: ●calculated from Eqs. (1)–(6), (8) and (9); ○ calculated from Eqs. (8) and (9), with $\gamma^{aq} = K_1 + K_2T$. Lines: trend lines.

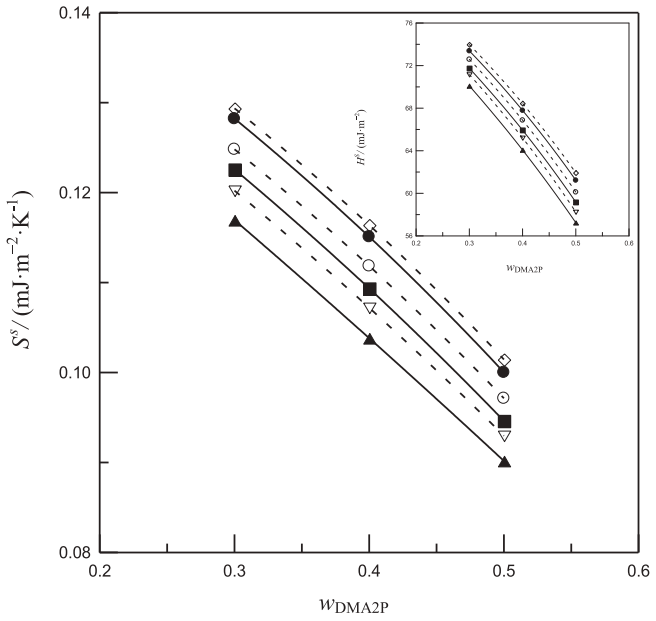


**Fig. 6.** $w_{DMA2P}$ dependence of the surface entropies and surface enthalpies (insert plot) of DMA2P-MEA (solid symbols and solid lines) and DMA2P-PZ (hollow symbols and dashed lines) aqueous solutions. ●$w_{MEA}$ = 0.05; ■$w_{MEA}$ = 0.10; ▲$w_{MEA}$ = 0.15; ◇$w_{PZ}$ = 0.025; ○$w_{PZ}$ = 0.05; ▽$w_{PZ}$ = 0.075. Symbols: calculated from Eqs. (1)–(6), (8) and (9). Lines: trend lines.

(3) The proposed equation can correctly capture the effects of temperature and mass fractions of amines on the surface tension, and the calculated results agree well with the experimental results;
(4) The surface entropy and surface enthalpy of DMA2P aqueous solutions firstly decrease and then increase rapidly at the water-poor region. Those of DMA2P-MEA and DMA2P-PZ aqueous solutions decrease with increasing mass fractions

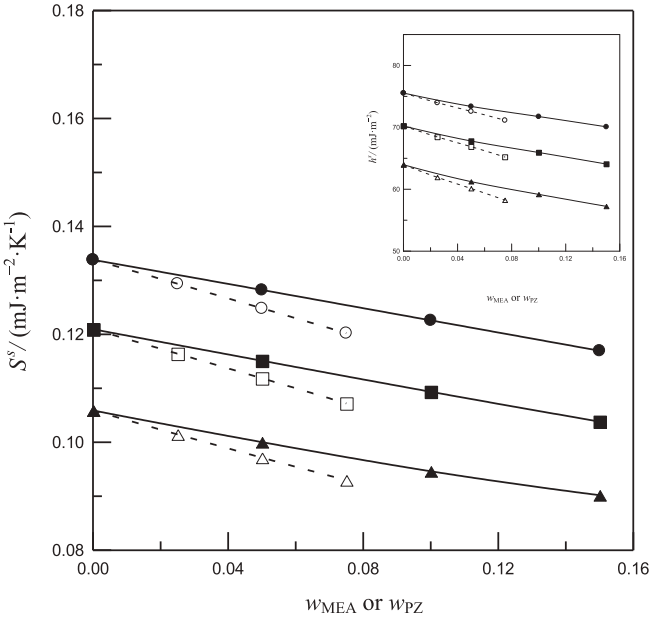


**Fig. 7.** $w_{\mathrm{MEA}}$ or $w_{\mathrm{PZ}}$ dependence of the surface entropies and surface enthalpies (insert plot) of DMA2P-MEA (solid symbols and solid lines) and DMA2P-PZ (hollow symbols and dashed lines) aqueous solutions. Symbols: calculated from Eqs. (1)–(6), (8) and (9), ●○$w_{\mathrm{DMA2P}}$ = 0.3; ■□ $w_{\mathrm{DMA2P}}$ = 0.4; ▲△ $w_{\mathrm{DMA2P}}$ = 0.5. Lines: trend lines.

of amines, and PZ is able to decrease the surface thermodynamics of DMA2P aqueous solutions much more significantly than MEA.

## Acknowledgments

The authors appreciate the financial support from the National Natural Science Foundation of China (No. 21276072) and the Fundamental Research Funds for the Central Universities (13ZD16 and 2016XS108).

## References

[1] G.R. Dickens, Nature 429 (2004) 513–515.
[2] H. Herzog, Environ. Sci. Technol. 35 (2001) 148A–153A.
[3] A.B. Rao, E.S. Rubin, Environ. Sci. Technol. 36 (2002) 4467–4475.
[4] G.T. Rochelle, Science 325 (2009) 1652–1654.
[5] H. Yang, Z. Xu, M. Fan, R. Gupta, R.B. Slimane, A.E. Bland, I. Wright, J. Environ. Sci. 20 (2008) 14–27.
[6] A.L. Kohl, R. Nielsen, Gas Purification, Gulf Professional Publishing, 1997.
[7] S. Kim, H. Shi, J.Y. Lee, Int. J. Greenhouse Gas Control 45 (2016) 181–188.
[8] M. Wang, A. Lawal, P. Stephenson, J. Sidders, C. Ramshaw, Chem. Eng. Res. Des. 89 (2011) 1609–1624.
[9] P. Derks, H. Dijkstra, J. Hogendoorn, G. Versteeg, AIChE J. 51 (2005) 2311–2327.
[10] J.M. Navaza, D. Gómez-Díaz, M.D. La Rubia, Chem. Eng. J. 146 (2009) 184–188.
[11] R. Idem, M. Wilson, P. Tontiwachwuthikul, A. Chakma, A. Veawab, A. Aroonwilas, D. Gelowitz, Ind. Eng. Chem. Res. 45 (2006) 2414–2420.
[12] M. Haji-Sulaiman, M. Aroua, A. Benamor, Chem. Eng. Res. Des. 76 (1998) 961–968.
[13] A. Haghtalab, E. Ghahremani, Fluid Phase Equilib. 400 (2015) 62–75.
[14] T. Chakravarty, U. Phukan, R. Weilund, Chem. Eng. Prog. 81 (1985) 32–36.
[15] B. Mandal, M. Guha, A. Biswas, S. Bandyopadhyay, Chem. Eng. Sci. 56 (2001) 6217–6224.
[16] C.Y. Lin, A.N. Soriano, M.H. Li, J. Taiwan Inst. Chem. E. 40 (2009) 403–412.
[17] P. Derks, J. Hogendoorn, G. Versteeg, J. Chem. Thermodyn. 42 (2010) 151–163.
[18] F.A. Chowdhury, H. Yamada, T. Higashii, K. Goto, M. Onoda, Ind. Eng. Chem. Res. 52 (2013) 8323–8331.
[19] S. Kadiwala, A.V. Rayer, A. Henni, Chem. Eng. J. 179 (2012) 262–271.
[20] L. Wen, H. Liu, W. Rongwong, Z. Liang, K. Fu, R. Idem, P. Tontiwachwuthikul, Chem. Eng. Technol. 38 (2015) 1435–1443.
[21] H. Liu, X. Luo, Z. Liang, P. Tontiwachwuthikul, Ind. Eng. Chem. Res. 54 (2015) 4709–4716.
[22] Y. Liang, H. Liu, W. Rongwong, Z. Liang, R. Idem, P. Tontiwachwuthikul, Fuel 144 (2015) 121–129.
[23] Z. Idris, L. Ang, D.A. Eimer, J. Ying, J. Chem. Eng. Data 60 (2015) 1419–1425.
[24] A.V. Rayer, A. Henni, Ind. Eng. Chem. Res. 53 (2014) 4953–4965.
[25] H. Liu, Y. Liang, Z. Liang, S. Liu, K. Fu, T. Sema, W. Rongwong, Energy Procedia 63 (2014) 659–664.
[26] D. Fu, Y.F. Xu, L.F. Wang, L.H. Chen, Sci. China Chem. 55 (2012) 1467–1473.
[27] D. Fu, Y.F. Xu, X.Y. Hua, Fluid Phase Equilib. 314 (2012) 121–127.
[28] Y. Maham, A. Chevillard, A.E. Mather, J. Chem. Eng. Data 49 (2004) 411–415.
[29] Y. Maham, A. Mather, Fluid Phase Equilib. 182 (2001) 325–336.
[30] J. Aguila-Hernández, A. Trejo, J. Gracia-Fadrique, Fluid Phase Equilib. 185 (2001) 165–175.
[31] E. Alvarez, R. Rendo, B. Sanjurjo, M. Sanchez-Vilas, J.M. Navaza, J. Chem. Eng. Data 43 (1998) 1027–1029.
[32] G. Vázquez, E. Alvarez, J.M. Navaza, R. Rendo, E. Romero, J. Chem. Eng. Data 42 (1997) 57–59.
[33] G. Vázquez, E. Alvarez, R. Rendo, E. Romero, J.M. Navaza, Chem. Eng. Data 41 (1996) 806–808.
[34] D. Fu, H.M. Wang, L.X. Du, J. Chem. Thermodyn. 71 (2014) 1–5.
[35] D. Fu, L.X. Du, H.M. Wang, J. Chem. Thermodyn. 69 (2014) 132–136.
[36] D. Fu, L. Wei, S.T. Liu, Fluid Phase Equilib. 337 (2013) 83–88.
[37] D. Fu, F. Liu, Z. Li, Chem. Eng. Technol. 36 (2013) 1859–1864.
[38] D. Fu, Z.K. Zhong, Acta Chim. Sinica 68 (2010) 1241–1246.
[39] J. Águila-Hernández, A. Trejo, B.E. García-Flores, Colloids Surf., A 308 (2007) 33–46.
[40] J. Gliński, G. Chavepeyer, J.K. Platten, J. Chem. Phys. 114 (2001) 5702–5706.
[41] J. Glinski, G. Chavepeyer, J.K. Platten, J. Chem. Phys. 111 (1999) 3233–3236.
[42] J. Gliński, G. Chavepeyer, J.K. Platten, P. Smet, J. Chem. Phys. 109 (1998) 5050–5053.
[43] J. Gliński, G. Chavepeyer, J.K. Platten, J. Chem. Phys. 102 (1995) 2113–2117.
[44] A. Adamson, Physical Chemistry of Surfaces, fifth ed., Interscience, New York, 1990.
[45] R.S. Hansen, J. Phys. Chem. 66 (1962) 410–415.
[46] M.J.A. Barbas, F.A. Dias, A.F. Mendonça, I.M. Lampreia, Phys. Chem. Chem. Phys. 2 (2000) 4858–4863.

JCT 16-867